Am J Cancer Res 2026;16(8):3542-3555
www.ajcr.us /ISSN:2156-6976/ajcr0174698

Original Article

Dynamic changes in D-dimer during first-line therapy and their association with overall survival in advanced lung cancer: a retrospective study

Xiaoqiang Ye, Chengying Xu, Liyang Yu, Bicui Zhan

Department of Clinical Laboratory, Hangzhou TCM Hospital Affiliated to Zhejiang Chinese Medical University, Hangzhou 310007, Zhejiang, China

Received June 11, 2026; Accepted July 27, 2026; Epub August 15, 2026; Published August 30, 2026

Abstract: This study investigated the association between dynamic changes in D-dimer (D-D) during first-line systemic therapy and overall survival (OS) in patients with advanced lung cancer (LC). We also evaluated the independent prognostic value of these dynamic changes after adjusting for confounders and other coagulation markers. This retrospective study included patients with advanced LC who received first-line systemic therapy between January 2018 and December 2023. The percentage change in D-D from baseline to 3 months was calculated. A 3-month landmark analysis was used to reduce immortal time bias. We fitted multivariable Cox proportional-hazards models adjusted for age, sex, disease stage, histology, liver metastasis, and additional confounders (thrombosis history, hypertension, diabetes, chronic obstructive pulmonary disease [COPD], and anemia) to assess the independent association between D-D dynamics and OS. Combined models incorporating D-D, fibrinogen, and platelet data were also evaluated. Restricted cubic splines were utilized to validate the threshold selection. Model performance was evaluated using time-dependent receiver operating characteristic curves, calibration plots, and decision curve analysis. A nomogram for individualized prediction was derived from the combined model and internally validated by bootstrap calibration. Among 192 enrolled patients, the landmark cohort comprised 160 cases (median follow-up 32.5 months). The D-D increase group had a significantly shorter median OS than the stable groups (8.2 vs. 51.8 months) and the decrease group (median not reached; log-rank $P < 0.001$). After full adjustment, a marked D-D increase remained independently associated with a higher risk of death compared with the stable group (HR = 2.60, 95% CI: 1.44-4.71, $P = 0.002$), whereas a marked decrease showed a protective trend (HR = 0.56, 95% CI: 0.29-1.08, $P = 0.084$). The combined model that included D-D dynamics, fibrinogen changes, and platelet status achieved a C-index of 0.697, outperforming the D-D-only model (0.667) and the clinical-only model (0.592). Dynamic D-D changes are independently associated with OS in advanced LC during first-line treatment. The combined model, presented as a practical nomogram, offers a tool for individualized risk stratification; however, external multicenter validation is warranted.

Keywords: Advanced lung cancer, D-dimer, dynamic change, prognosis, landmark analysis

Introduction

Lung cancer (LC) is one of the most prevalent and deadly malignancies worldwide. According to the GLOBOCAN 2022 report, its incidence and mortality rates are among the highest of all cancers [1]. Non-small cell LC (NSCLC) accounts for approximately 80%-85% of all LC cases, and most patients are already diagnosed at an advanced stage [2]. Although targeted agents, immunotherapies, and anti-angiogenic drugs have improved survival, the 5-year overall survival (OS) rate remains unsatisfactory [3]. Therefore, it is critical to find easily measurable, dynamic, and reproducible prognostic biomarkers.

Cancer frequently activates the coagulation cascade [4]. D-dimer (D-D) is a degradation product of cross-linked fibrin and serves as a key marker of coagulation activation and subsequent fibrinolysis. Substantial evidence links elevated baseline D-D levels to poor prognosis in LC [5-7]. Additionally, high pre-treatment D-D levels have been shown to be associated with poor survival after first-line immunotherapy in

https://doi.org/10.62347/VZHI7640

NSCLC [8]. The D-D ratio, combined with other parameters, has also been validated as a valuable prognostic marker in small cell LC (SCLC) [6, 9]. In extensive-stage SCLC, high pre-treatment D-D values correlated with poor survival [10]. More recent studies have indicated an association between D-D and tumor genetic mutation status [11].

However, most current studies have measured D-D at a single pre-treatment time point [12, 13]. Longitudinal data on D-D changes during first-line therapy and their incremental prognostic value for longer-term survival remain limited. In particular, systematic evaluations are lacking regarding (1) the optimal cutoff values for defining clinically meaningful D-D changes; (2) whether dynamic D-D changes provide information independent of baseline levels; and (3) the feasibility of developing a simple risk-stratification tool based on D-D dynamics. Addressing these questions may facilitate early identification of high-risk patients and guide dynamic treatment adjustments in clinical practice.

In this context, the present study aimed to systematically evaluate the independent association of D-D dynamics during first-line therapy with OS in advanced LC, using a retrospective cohort design. We performed a landmark analysis to minimize immortal time bias. The thresholds for categorizing D-D changes were validated using restricted cubic splines (RCS). Multivariable Cox regression models were used to assess the independent prognostic significance of D-D change categories (decrease, stable, increase). Furthermore, a predictive model incorporating D-D dynamics was built and internally validated, with the goal of providing a simple, clinically accessible tool for risk stratification.

Materials and methods

Study population

We included consecutive patients with pathologically confirmed advanced LC who received first-line systemic therapy at the Department of Oncology of Hangzhou TCM Hospital Affiliated to Zhejiang Chinese Medical University between January 2018 and December 2023. A total of 192 patients were initially included.

Inclusion criteria: age ≥ 18 years; histologically or cytologically proven NSCLC or SCLC with clinical stage IIIB/IV or unresectable recurrent disease [14]; first-line systemic therapy (chemotherapy, immunotherapy, targeted therapy, or anti-angiogenic therapy); and complete survival follow-up data. Exclusion criteria: presence of another active malignancy; use of anticoagulant or antiplatelet agents within 3 months prior to enrolment; or critically missing clinical information.

The study protocol was approved by the Ethics Committee of Hangzhou TCM Hospital Affiliated to Zhejiang Chinese Medical University (Approval No. 2026KLL091). Due to the retrospective design, the requirement for informed consent was waived by the ethics committee.

Data collection

The following baseline information was retrieved from electronic medical records: age, sex, histological subtype (adenocarcinoma, squamous cell carcinoma, or small cell carcinoma), TNM stage (IIIB vs. IV), and first-line therapy regimen. The sites of distant metastases (bone, liver, brain, etc.) were also recorded.

Coagulation parameters included D-D, fibrinogen (Fb), prothrombin time (PT), activated partial thromboplastin time (APTT), international normalized ratio (INR), and platelet count. The percentage change in D-D was calculated as (post-treatment value - pre-treatment value)/pre-treatment value × 100%.

The primary endpoint was OS, defined as the time from start of first-line therapy until death from any cause or last follow-up [15]. The secondary endpoint was progression-free survival which was defined as the time from initiation of treatment to progression of disease or death.

Statistical analysis

All statistical analyses were performed using R software (version 4.5.2). Normally distributed continuous variables are presented as mean ± standard deviation and compared between groups using independent-samples t-tests. Non-normally distributed continuous variables are presented as median with interquartile range (IQR) and compared using the Mann-Whitney U test. Categorical variables are expressed as numbers and percentages and compared using the χ^2 test or Fisher's exact test, as appropriate.

To reduce immortal time bias, we conducted a landmark analysis at 3 months after treatment initiation; patients who died before this time point were excluded, and all subsequent survival analyses were based on the landmark dataset. The dose-response relationship between D-D percentage change and mortality risk was evaluated using RCS analysis. Based on previous literature [16] and model fit, D-D dynamics were classified into three categories: decrease (change < -25%), stable (change between -25% and 50%), and increase (change > 50%). Fibrinogen changes were similarly categorized as decreased (< -25%), stable (-25% to 25%), or increased (> 25%).

The following variables were included in the multivariable Cox proportional-hazards model: age, sex, stage (IV vs. IIIB), histology (small cell carcinoma vs. non-small cell carcinoma), liver metastasis (present vs. absent), and dynamic D-D change category (stable group as reference). Multicollinearity was tested using variance inflation factors (VIF), and no significant collinearity was detected (all VIF < 5). Schoenfeld residuals were used to verify the proportional-hazards assumption.

Harrell's C-index was used for assessing model discrimination. Time-dependent receiver operating characteristic (ROC) curves were generated at 6, 12, and 18 months to assess predictive accuracy at each time point. Calibration was assessed using calibration plots with 1,000 bootstrap resamples, and the mean absolute error (MAE) was reported. Decision curve analysis (DCA) was carried out to estimate clinical net benefit. The final model was internally validated via 1,000 bootstrap resamples to obtain an optimism-corrected C-index with 95% confidence interval (CI).

Net benefit was evaluated across threshold probabilities from 5% to 95% to provide a comprehensive view of clinical utility.

Subgroup analyses were performed according to the presence or absence of bone and liver metastases. Multivariable Cox models were used to assess whether the association between D-D dynamics and survival differed by metastasis status; a P > 0.05 value for the interaction term indicated no significant difference.

Two types of sensitivity analyses were performed. First, the baseline D-D level was included in the model to determine whether D-D dynamics remained independent of baseline values. Second, the D-D change groups were redefined using symmetric thresholds of ±20% and ±30%, and model fit (Akaike information criterion, AIC) and C-index were compared with the original threshold scheme to assess robustness. All tests were two-tailed, and a *P* value < 0.05 was considered statistically significant.

To address potential confounding, an extended multivariable model additionally adjusted for thrombosis history, hypertension, diabetes, chronic obstructive pulmonary disease (COPD), and anemia, based on their clinical relevance to coagulation and survival. A combined prediction model that incorporated D-D change categories, fibrinogen change categories, and baseline platelet status [thrombocytosis (> 300 × 10^9/L) vs. normal] was constructed and compared with the D-D-only model using Harrell's C-index and AIC. Furthermore, subgroup analyses were extended to include stratification by histology, first-line treatment regimen, and disease stage. A nomogram was constructed from the combined coagulation-marker Cox model to provide a visual tool for predicting individual overall survival probabilities. Points were assigned to each predictor according to its regression coefficient, and total points were converted into linear predictors and then into 1-, 2-, and 3-year overall survival probabilities using the baseline survival function. Internal validation of the nomogram was performed with 1,000 bootstrap resamples, and a bootstrap calibration plot at 3 years was generated to assess agreement between predicted and observed probabilities.

To characterize longitudinal coagulation profile beyond the single percentage-change metric, each patient was classified into one of four D-dimer trajectory patterns based on binary elevation status (cut-off 4.5 mg/L) at baseline and at 3 months: persistent-normal, new-onset-elevated, normalized, and persistent-high. For the combined coagulation-marker Cox model, an individualized risk score was derived from the model linear predictor; patients in the landmark cohort were divided into low-, intermediate-, and high-risk groups by tertiles, and sur-

Table 1. Baseline characteristics of the landmark cohort (N = 160)

Characteristic	Alive (n = 92)	Dead (n = 68)	P
Age (years), median [IQR]	64.0 [57.8-69.2]	65.0 [59.8-70.0]	0.347
Gender, n (%)			0.730
Male	71 (77.2)	50 (73.5)	
Female	21 (22.8)	18 (26.5)	
Histology, n (%)			0.115
Adenocarcinoma	54 (58.7)	27 (39.7)	
Squamous cell	15 (16.3)	11 (16.2)	
Small cell	23 (25.0)	25 (36.8)	
Others	0 (0.0)	5 (7.4)	
Stage, n (%)			0.284
IIIB	4 (4.3)	4 (5.9)	
IV	76 (82.6)	52 (76.5)	
Unresectable recurrence	12 (13.0)	12 (17.6)	
Liver metastasis, n (%)			0.017
Yes	8 (8.7)	16 (23.5)	
No	84 (91.3)	52 (76.5)	
Bone metastasis, n (%)			0.288
Yes	30 (32.6)	21 (30.9)	
No	62 (67.4)	47 (69.1)	
Treatment type, n (%)			0.871
Chemotherapy/others	25 (27.2)	16 (23.5)	
Immunotherapy	42 (45.7)	36 (52.9)	
Targeted therapy	25 (27.2)	16 (23.5)	
Baseline platelet ($\times 10^9$/L), median [IQR]	264.1 [220.0-310.3]	222.9 [171.9-271.0]	0.004
D-D change (%), median [IQR]	-6.7 [-24.1-23.7]	17.2 [-14.4-45.5]	0.005

Note: IQR, interquartile range; D-D, D-dimer.

vival differences were assessed by log-rank test.

Results

Baseline characteristics and dynamic changes in coagulation parameters

Initially, 192 patients with advanced LC were enrolled. After the 3-month landmark, 31 patients who died within the first 3 months and one patient with unknown stage were excluded, leaving 160 patients for analysis. Of these, 68 died and 92 survived. The median follow-up time was 32.5 months (IQR 16.4-54.2 months).

In the landmark cohort, the proportion of patients with liver metastasis differed significantly between the deceased and alive groups (21.0% vs. 8.7%, P = 0.017). Baseline platelet count was also significantly lower in deceased patients than in survivors (median 222.9 vs. 264.1 × 10^9/L, P = 0.004). The median percentage change in D-D was significantly higher in deceased patients (17.2% vs. -6.7%, P = 0.005). No significant differences were observed between the two groups regarding age, sex, histology, stage, or treatment type (all P > 0.05). Detailed baseline characteristics are summarized in **Table 1**.

Univariate survival analysis

Kaplan-Meier curves showed a strong association between D-D change categories and OS (log-rank P < 0.001, **Figure 1**). The median OS was shortest in the increase group (8.2 months), followed by the stable group (51.8 months); median OS was not reached in the decrease group.

Reclassifying patients by their binary elevation status at baseline and 3 months yielded four trajectories: persistent-normal (n = 84), persis-

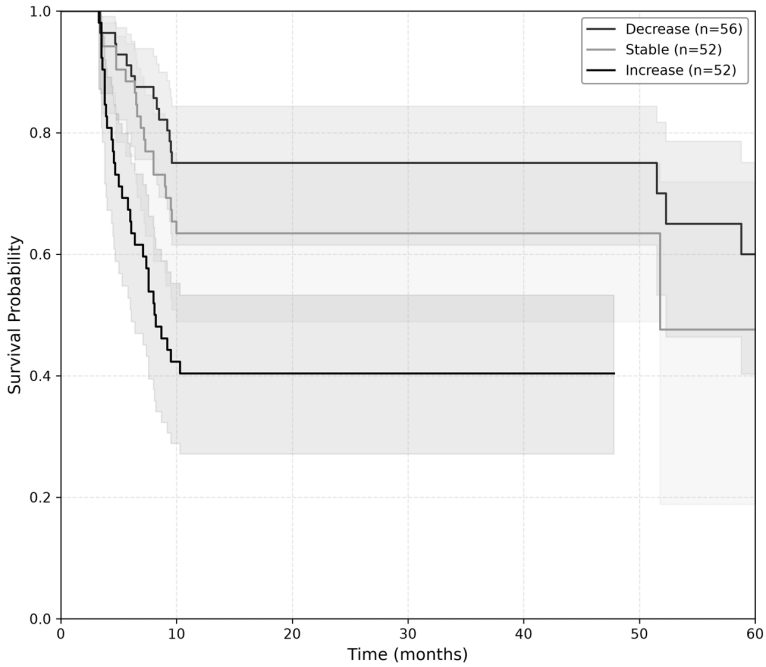

Figure 1. Kaplan-Meier survival curves for overall survival stratified by D-dimer change groups. The y-axis represents survival probability, and the x-axis represents time in months. Tick marks indicate censored observations.

tent-high (n = 81), normalized (n = 15), and new-onset-elevated (n = 12). Persistent-high pattern was associated with markedly worse survival (median OS 9.2 months) than persistent-normal or normalized patterns (median OS not reached), whereas new-onset-elevated pattern showed an intermediate and unfavorable course (median OS 6.0 months; adjusted HR 2.11, 95% CI 1.01-4.37, P = 0.046 versus persistent-normal). Across the whole cohort, persistent-high pattern versus all other patterns yielded a highly significant separation in OS (log-rank P < 0.001; **Figure 2**). These patterns indicate that sustained, rather than transient, hypercoagulability is the principal prognostic driver.

Univariate Cox regression showed that each 10% increment in D-D percentage change was associated with an approximately 11.9% higher risk of death (HR = 1.12, 95% CI: 1.04-1.20, P < 0.001). Using the stable group as reference, the increase group had a significantly elevated death risk (HR = 2.12, 95% CI: 1.20-3.74, P = 0.009), whereas the decrease group did not differ significantly from the stable group (HR = 0.64, 95% CI: 0.33-1.24, P = 0.186).

Multivariable Cox regression

In a multivariable Cox model adjusted for age, sex, stage, histology, and liver metastasis, a marked D-D increase remained independently associated with a higher risk of death compared with the stable group (HR = 2.57, 95% CI: 1.42-4.65, P = 0.002, **Figure 3**). The decrease group showed a protective trend, but it did not reach statistical significance (HR = 0.55, 95% CI: 0.28-1.08, P = 0.080). The global proportional-hazards assumption was satisfied (Schoenfeld residual test, P = 0.611), and each individual variable also met the assumption (Table S1). After further adjustment for additional confounders (thrombosis history, hypertension, diabetes, COPD, anemia), the D-D increase remained independently associated with mortality (HR = 2.60, 95% CI: 1.44-4.71, P = 0.002), confirming the robustness of this association. In the combined coagulation-marker model (which additionally included fibrinogen change groups and baseline platelet status), D-D increase remained significant (HR = 2.87, 95% CI: 1.54-5.36, P = 0.001), and a high platelet count was independently associated with better survival (HR = 0.39, 95% CI: 0.19-0.78, P = 0.008). The combined model achieved a C-index of 0.697, compared to 0.667 for the D-D-only model and 0.592 for the clinical-only model.

Model performance evaluation and validation

Model 2 (clinical factors + D-D change categories) had a Harrell's C-index of 0.667, higher than Model 1 (clinical factors only, C-index = 0.592, **Figure 4**). After internal validation with 1, 000 bootstrap resamples, the optimism-corrected C-index was 0.633 (95% CI: 0.622-0.757), suggesting stable discriminative ability. The combined model incorporating D-D, fibrinogen dynamics, and baseline platelet status yielded a further improved C-index of 0.697

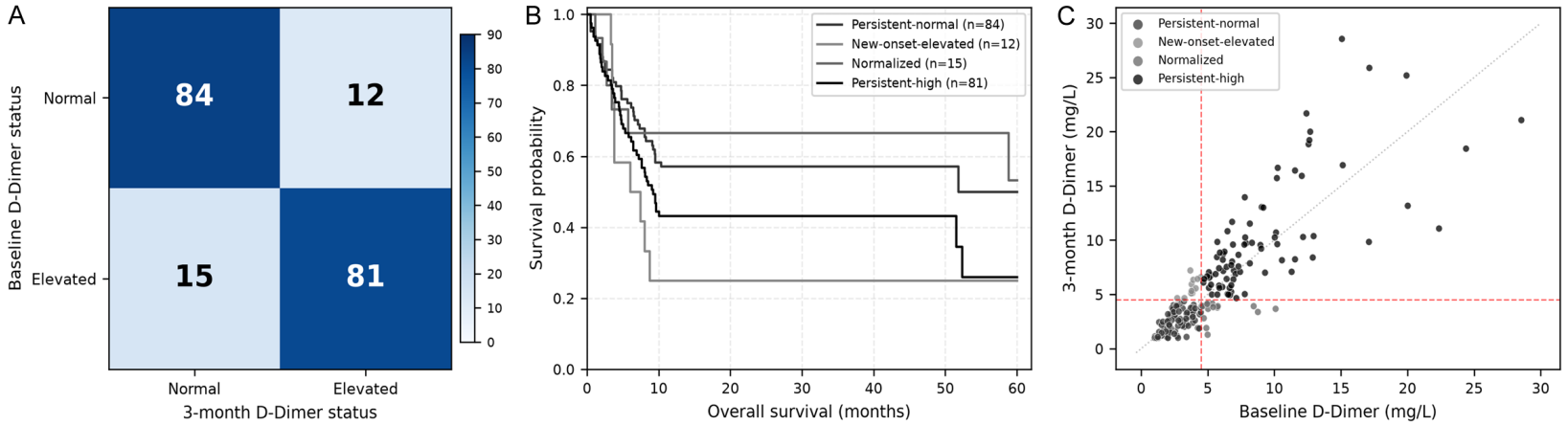

Figure 2. D-dimer trajectory patterns from baseline to 3 months. A. Transition matrix of D-dimer elevation status (cut-off 4.5 mg/L) between baseline and 3 months. B. Kaplan-Meier overall survival curves by trajectory pattern (log-rank P < 0.001). C. Paired scatter of baseline versus 3-month D-dimer levels; points are colored by trajectory pattern and the dashed line indicates equality.

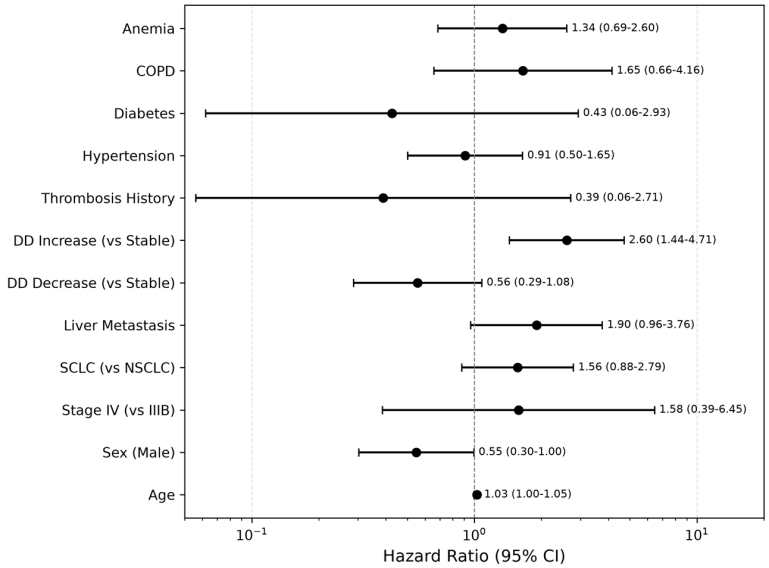

Figure 3. Forest plot of multivariable Cox regression analysis (extended model). Hazard ratios (HRs) with 95% confidence intervals are shown for each variable.

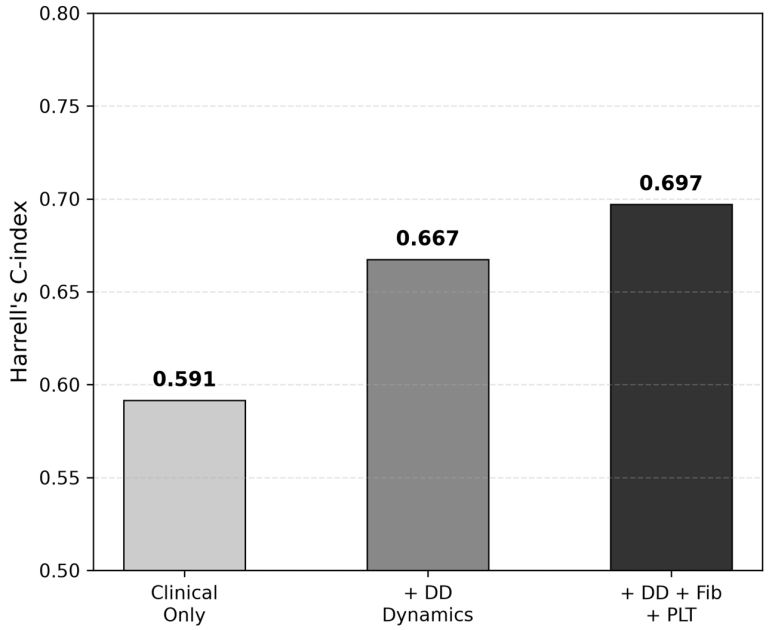

Figure 4. Comparison of model discrimination (Harrell's C-index) across three models: clinical-only, D-dimer-only, and combined coagulation-marker model.

(AIC = 623.8), outperforming both the clinical-only and D-D-only models.

Time-dependent ROC analysis demonstrated that the area under the curve (AUC) for predicting OS at 6, 12, and 18 months was 0.702, 0.713, and 0.713, respectively, for Model 2. The calibration curve showed good agreement between predicted and observed probabilities (MAE = 0.013, Figure S1). A modest difference in clinical net benefit between Model 2 and Model 1 was observed in the threshold probability range above 25% (**Figure 5**).

Nomogram for individual prediction

To translate the combined model into clinical practice, we constructed a nomogram incorporating age, sex, tumor stage, histology, liver metastasis, D-D and fibrinogen change categories, and baseline platelet status (**Figure 6**). The nomogram enables direct readout of the predicted 1-, 2-, and 3-year OS probabilities for individual patients. The bootstrap calibration plot at 3 years showed close agreement between predicted and observed OS probabilities (**Figure 7**), indicating satisfactory internal calibration.

Applying the combined-model risk score to the landmark cohort stratified patients into low- (n = 53), intermediate- (n = 53), and high-risk (n = 54) groups with clearly separated OS (log-rank P < 0.001; **Figure 8A**). Multi-timepoint calibration of the combined model showed close agreement between predicted and observed 6-, 9-, and 12-month survival probabilities (Figure S2). In decision curve analysis at 12 months, the nomogram provided positive net clinical benefit across threshold probabilities from approximately 10% to 60%, with net benefit comparable to a treat-all strategy at low thresholds and progressively lower than treat-all above about 50% (**Figure 8B**). Thus, the

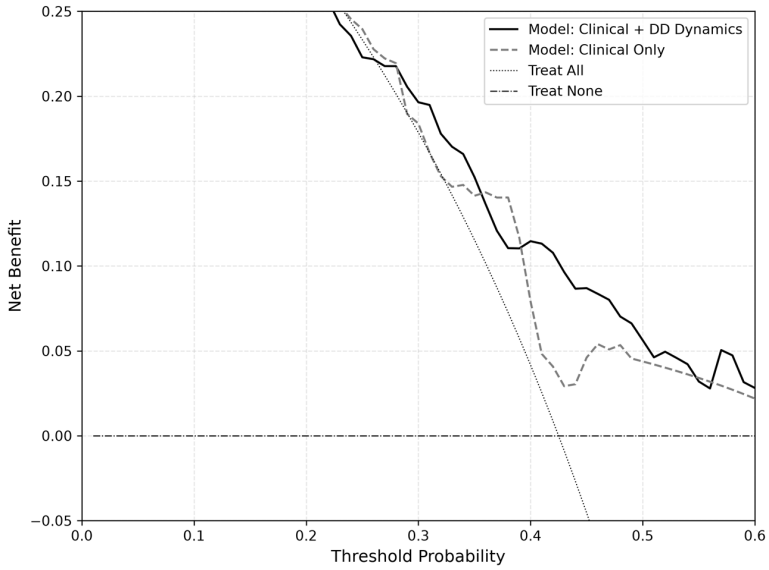

Figure 5. Decision curve analysis (DCA) for 12-month overall survival. DCA comparing the net benefit of different strategies for 12-month OS. The x-axis represents threshold probability, and the y-axis represents standardized net benefit. Model 2 shows a higher net benefit than Model 1 within threshold probabilities > 25%. The gray solid line represents the "Treat All" strategy, and the black dashed line represents the "Treat None" strategy.

combined model offers modest, threshold-dependent clinical utility that warrants external confirmation.

Sensitivity analysis

RCS analysis revealed a non-linear relationship between D-D percentage change and mortality risk, supporting -25% and +50% as suitable thresholds for categorization (Figure S3). Re-classification using symmetric thresholds of ±20% and ±30% resulted in a lower C-index and higher AIC than the original threshold scheme, suggesting robustness of our original classification.

Further adjustment for baseline D-D did not attenuate the association between D-D increase and death risk (HR = 2.56, 95% CI: 1.41-4.63, P = 0.002), suggesting that dynamic change provides prognostic information beyond baseline levels.

Subgroup analysis

Stratified analyses by bone and liver metastases revealed that the direction of the association between D-D dynamics and OS was generally consistent across subgroups. Extended subgroup analyses by histological demonstrated that D-D increase was most strongly associated with mortality in SCLC (HR = 3.62, P = 0.008) and adenocarcinoma (HR = 2.39, P = 0.016) (**Figure 9**). When stratified by first-line treatment regimen (**Figure 10**), D-D decrease showed a significant protective effect in patients receiving immunotherapy (HR = 0.37, P = 0.023) and chemotherapy (HR = 0.48, P = 0.044).

Relationship between D-D change and treatment response

The percentage change in D-D differed significantly across RECIST response categories (Kruskal-Wallis test, P < 0.001; Figure S4). The median D-D change was 45.8% in the progressive disease group, significantly higher than in the stable disease group (-6.2%) and the partial/complete response group (-32.0%). This finding suggests that a reduction in D-D is associated with better treatment response.

Discussion

In this retrospective study of 160 patients with advanced LC, we demonstrated that dynamic changes in D-D during first-line treatment were independently associated with OS. Specifically, an increase in D-D was an independent predictor of mortality (HR = 2.57), whereas a decrease showed a protective trend (HR = 0.55) compared with the stable group. These findings indicate that the direction of D-D change may provide prognostic information beyond the absolute value.

Compared with previous studies, our study makes several novel contributions. First, most earlier reports focused on a single pre-treatment D-D measurement, showing that elevated baseline levels are a poor prognostic predictor in LC and are associated with poor survival after first-line immunotherapy in NSCLC [8]. Our data suggest that D-D dynamics during treat-

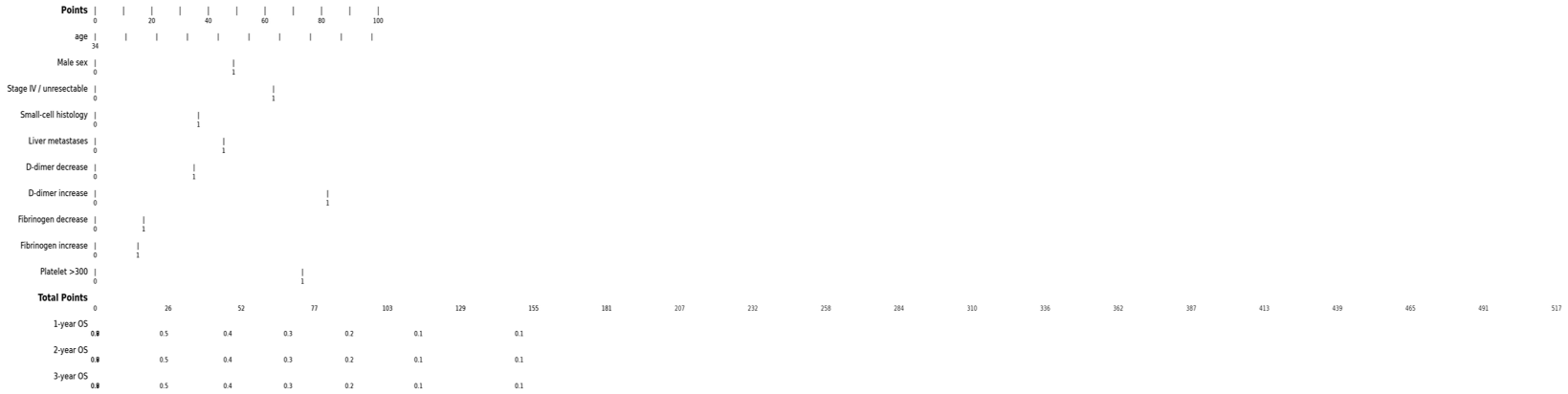

Figure 6. Nomogram for predicting overall survival based on the combined coagulation-marker model. Each variable is assigned a points score on the upper scale; total points are converted to predicted 1-, 2-, and 3-year overall survival probabilities.

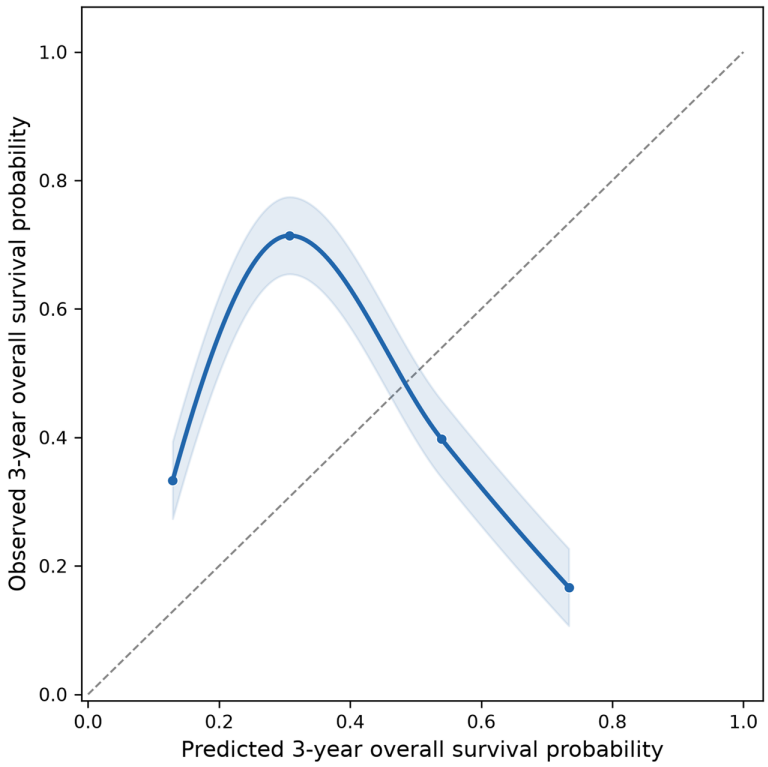

Figure 7. Bootstrap calibration plot of the nomogram at 3 years. The dashed line represents ideal prediction; the solid line represents the bootstrap-corrected observed probabilities.

ment have independent prognostic value comparable to, or even exceeding, that of baseline values. This is consistent with prior observations in EGFR-mutated patients, where D-D dynamics during EGFR-targeted therapy correlated with treatment response and disease progression [17]. Second, we used RCS analysis to validate the percentage change thresholds. We found that -25% and +50% cut-offs effectively distinguished risk groups and provided a better model fit than symmetric thresholds of ±20% and ±30%. These cut-offs are broadly similar to previously reported values [15] and offer a quantitative basis for monitoring D-D dynamics in routine practice. Third, the independent association of D-D dynamics with survival persisted after adjustment for baseline D-D levels. This observation reinforces that the change itself carries prognostic significance regardless of baseline levels, and that on-treatment dynamics may be more informative than a single pre-treatment assessment.

Notably, the D-D decrease group had better survival than the stable group, in line with earlier reports that normalization of elevated D-D predicts favorable prognosis [10]. This further supports using D-D reduction during treatment as an early indicator of treatment efficacy. Among the coagulation parameters examined, D-D dynamics appeared to be the most prominent independent prognostic factor, consistent with the recognized prognostic role of coagulation markers in LC [18].

The following mechanistic interpretation is based on established literature rather than on direct experimental validation in the present cohort. The mechanistic link between persistently elevated D-D and poor prognosis can be understood through a multifaceted framework involving coagulation, inflammation, angiogenesis, and tumor biology. First, the tissue factor/protease-activated receptor (PAR) signaling pathway drives coagulation activation and promotes tumor proliferation [19, 20]. Second, coagulation proteases and PAR signaling promote cancer immune evasion and sustain a tumor-promoting microenvironment [20, 21]. Third, fibrin degradation products sequester angiogenic factors such as vascular endothelial growth factor (VEGF) and basic fibroblast growth factor (bFGF), thereby enhancing neovascularization [21, 22]. Fourth, sustained D-D elevation may reflect occult thromboembolic events and circulating procoagulant microparticles that impair microvascular drug delivery [23].

Clinically, all variables in our study are derived from routine laboratory tests, making them readily available, inexpensive, and reproducible. A simple risk score based on D-D dynamics is advantageous because of its simplicity and dynamic availability. This approach parallels previous strategies that built prognostic models using multidimensional indicators [24]. DCA confirmed that this score provided net clin-

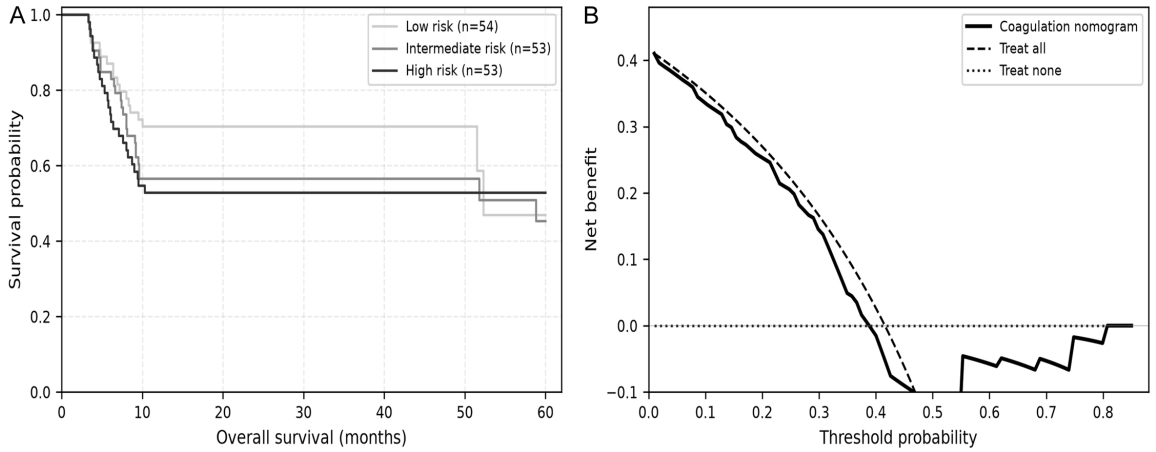

Figure 8. Clinical utility of the combined coagulation-marker model. A. Kaplan-Meier overall survival by risk-score tertile (low/intermediate/high; log-rank P < 0.001). B. Decision curve analysis for 12-month overall survival; the nomogram (solid) is compared with treat-all (dashed) and treat-none (dotted) strategies across threshold probabilities.

ical benefit across a range of threshold probabilities. For patients with a higher risk score, one might consider more frequent imaging follow-up, proactive management of thrombotic risk, earlier efficacy assessment, or treatment modification.

Several limitations should be acknowledged. First, this was a single-center retrospective cohort study, which carries inherent risks of information and selection bias. Data extracted from electronic medical records may contain inaccuracies and coding inconsistencies. Second, D-D assays vary across reagents, calibrators, and laboratory platforms, introducing potential detection bias. Third, the limited sample size reduced statistical power for subgroup analyses. Fourth, D-D and fibrinogen were measured at only two time points; two-point sampling cannot fully depict the longitudinal coagulation trajectory or distinguish transient elevation from persistent hypercoagulability. Serial prospective measurements are warranted. The trajectory classification demonstrates that persistent hypercoagulability - not transient fluctuation - drives prognosis, which partly addresses this limitation. Fifth, although we developed a visual nomogram based on the combined coagulation-marker model to facilitate bedside risk stratification, the model lacked independent external validation, and its predictive performance requires confirmation in external cohorts. Sixth, the mechanistic links discussed above (coagulation-inflammation-angiogenesis crosstalk, tissue factor/protease-activated receptor signaling, and fibrin-degradation-product-mediated VEGF sequestration) are based on existing literature rather than direct experimental validation in the this cohort; dedicated basic research is needed to substantiate these pathways. Seventh, we could not fully account for unmeasured confounders, such as performance status, comprehensive comorbidity indices, and tumor genetic mutation status.

Conclusion

In summary, dynamic changes in D-D are independently associated with OS in patients with advanced LC receiving first-line treatment. A marked increase portends a worse prognosis, whereas a marked decrease is associated with improved survival. The D-D dynamics-based risk stratification model may serve as a complementary tool to conventional imaging for identifying high-risk patients. Nevertheless, these findings are preliminary; prospective multicenter studies are needed to validate the clinical utility of this approach.

Acknowledgements

This study was supported by the General Project of Hangzhou Health Science and Technology Program (No. A20260818) and the 2024 Hangzhou Agriculture and Social Development Project (No. 20241029Y059).

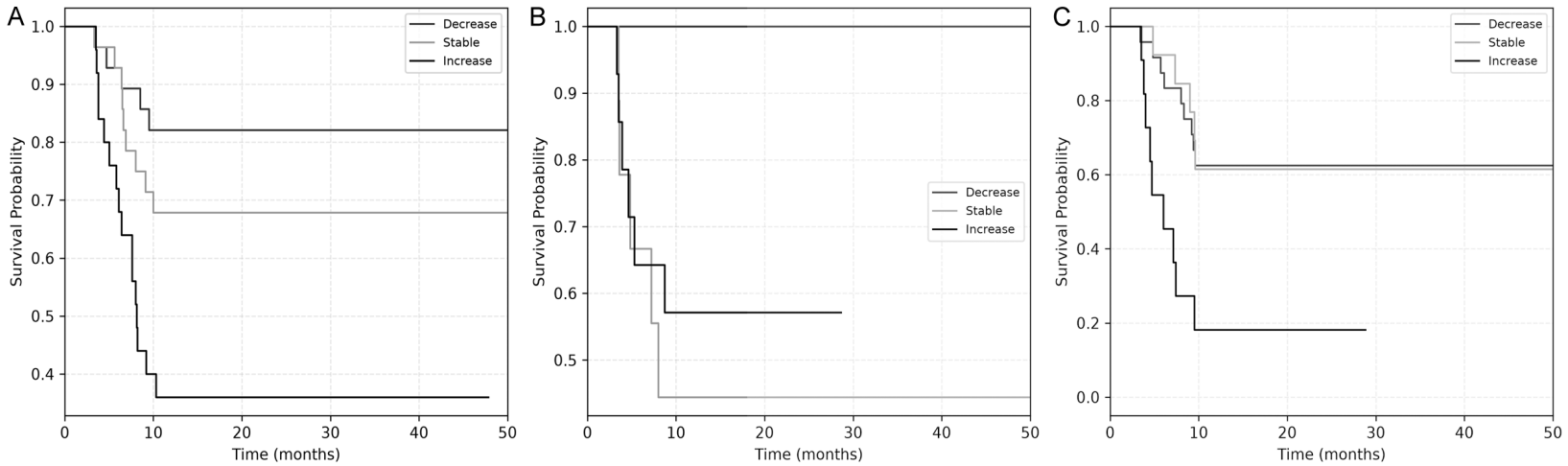

Figure 9. Kaplan-Meier survival curves stratified by histological type: (A) adenocarcinoma, (B) squamous cell carcinoma, (C) small cell lung cancer.

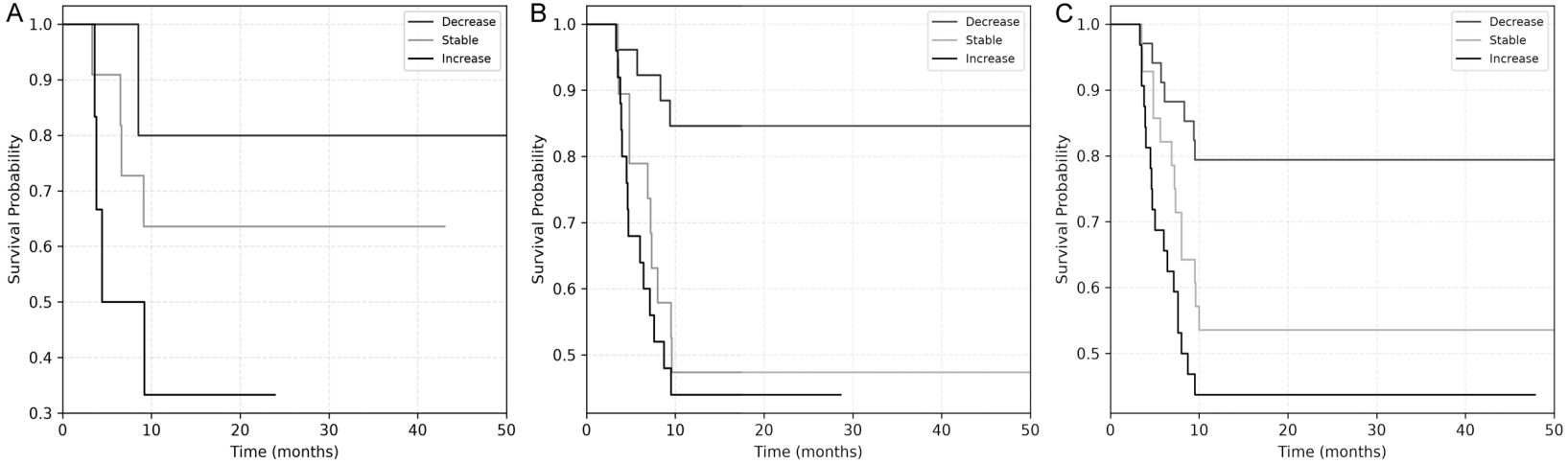

Figure 10. Kaplan-Meier survival curves stratified by first-line treatment regimen: (A) targeted therapy, (B) immunotherapy, (C) chemotherapy/other.

Disclosure of conflict of interest

None.

Address correspondence to: Bicui Zhan, Department of Clinical Laboratory, Hangzhou TCM Hospital Affiliated to Zhejiang Chinese Medical University, No. 453 Tiyuchang Road, Hangzhou 310007, Zhejiang, China. E-mail: bcnzbc@163.com

References

[1] Zhou J, Xu Y, Liu J, Feng L, Yu J and Chen D. Global burden of lung cancer in 2022 and projections to 2050: incidence and mortality estimates from GLOBOCAN. Cancer Epidemiol 2024; 93: 102693.

[2] Abughanimeh O, Kaur A, El Osta B and Ganti AK. Novel targeted therapies for advanced non-small lung cancer. Semin Oncol 2022; 49: 326-336.

[3] Fortman D and Qin A. An evolving landscape: predictive and therapeutic biomarkers in advanced non-small cell lung cancer. Front Oncol 2026; 16: 1750153.

[4] Myrou A, Penopoulos A, Barmpagiannos K, Ouzouni S and Girtovitis F. Coagulation abnormalities in lung cancer: diagnostic challenges and therapeutic perspectives. Clin Appl Thromb Hemost 2025; 31: 10760296251359293.

[5] Ma M, Cao R, Wang W, Wang B, Yang Y, Huang Y, Zhao G and Ye L. The D-dimer level predicts the prognosis in patients with lung cancer: a systematic review and meta-analysis. J Cardiothorac Surg 2021; 16: 243.

[6] Li J, Wang Y, Li J and Che G. Prognostic value of pretreatment D-dimer level in small-cell lung cancer: a meta-analysis. Technol Cancer Res Treat 2021; 20: 1533033821989822.

[7] Deng HY, Ma XS, Zhou J, Wang RL, Jiang R and Qiu XM. High pretreatment D-dimer level is an independent unfavorable prognostic factor of small cell lung cancer: a systematic review and meta-analysis. Medicine (Baltimore) 2021; 100: e25447.

[8] Chen C, Yin H, Zhang Y, Chen H, Xu J and Ren L. Plasma D-dimer and interleukin-6 are associated with treatment response and progression-free survival in advanced NSCLC patients on anti-PD-1 therapy. Cancer Med 2023; 12: 15831-15840.

[9] Yao Y, Li X, Chen Z, Wu R, Wang B, Sun J, Miao L and Liu H. An exploratory ImmunoScore based on early on-treatment changes in NLR and LDH in small-cell lung cancer receiving first-line chemoimmunotherapy. Future Oncol 2026; 22: 1815-1828.

[10] Zhu LR, Li J, Chen P, Jiang Q and Tang XP. Clinical significance of plasma fibrinogen and D-dimer in predicting the chemotherapy efficacy and prognosis for small cell lung cancer patients. Clin Transl Oncol 2016; 18: 178-88.

[11] Chang F, Zhang H, Chen C, Ke Z, Zhao M, Fan X and Zhang Y. Concomitant genetic alterations are associated with plasma D-dimer level in patients with non-small-cell lung cancer. Future Oncol 2022; 18: 679-690.

[12] Abbas M, Kassim SA, Wang ZC, Shi M, Hu Y and Zhu H. Clinical evaluation of plasma coagulation parameters in patients with advanced-stage non-small cell lung cancer treated with palliative chemotherapy in China. Int J Clin Pract 2020; 74: e13619.

[13] Zhang Y, Cao J, Deng Y, Huang Y, Li R, Lin G, Dong M and Huang Z. Pretreatment plasma fibrinogen level as a prognostic biomarker for patients with lung cancer. Clinics (Sao Paulo) 2020; 75: e993.

[14] Wood DE. National Comprehensive Cancer Network (NCCN) clinical practice guidelines for lung cancer screening. Thorac Surg Clin 2015; 25: 185-97.

[15] Reitter EM, Kaider A, Ay C, Quehenberger P, Marosi C, Zielinski C and Pabinger I. Longitudinal analysis of hemostasis biomarkers in cancer patients during antitumor treatment. J Thromb Haemost 2016; 14: 294-305.

[16] Zhang L, Li X, Wang Z, Zhang Z, Zhang L, Liu Z, Zhang L, Wang S, Khorobrykh TV, He M and Xiao J. Albumin-to-D-dimer ratios: a novel prognostic factor for evaluating first-line chemotherapy efficacy in advanced lung adenocarcinoma patients. Neoplasma 2024; 71: 77-87.

[17] Li X, Lu D, Zhang Z, Zhang Y, Wang J and Hu Y. Prognostic value of plasma D-dimer levels in advanced non-small cell lung cancer patients treated with immune checkpoint inhibitors: a retrospective study. J Thorac Dis 2022; 14: 4125-4135.

[18] Luo Y, Lin K, Zhang M, Goto T, Brueckl WM, Lin J, Liu X, Weng J and Ye Y. Combination of the platelet-to-lymphocyte ratio and fibrinogen may predict 5-year overall survival of patient in non-small cell lung cancer treated with surgery. J Thorac Dis 2023; 15: 6967-6975.

[19] Kasthuri RS, Taubman MB and Mackman N. Role of tissue factor in cancer. J Clin Oncol 2009; 27: 4834-8.

[20] Paul S, Mukherjee T and Das K. Coagulation protease-driven cancer immune evasion: potential targets for cancer immunotherapy. Cancers (Basel) 2024; 16: 1568.

[21] Ma L, Perini R, McKnight W, Dicay M, Klein A, Hollenberg MD and Wallace JL. Proteinase-activated receptors 1 and 4 counter-regulate endostatin and VEGF release from human platelets. Proc Natl Acad Sci U S A 2005; 102: 216-20.

[22] Kwaan HC and Lindholm PF. Fibrin and fibrinolysis in cancer. Semin Thromb Hemost 2019; 45: 413-422.
[23] Thaler J, Ay C, Weinstabl H, Dunkler D, Simanek R, Vormittag R, Freyssinet JM, Zielinski C and Pabinger I. Circulating procoagulant microparticles in cancer patients. Ann Hematol 2011; 90: 447-53.
[24] Bai X, Wang X, Xu H, Bai Y, Chen Q, Bi S, Chen S, Yang H, Zhang X, Li F, Liu L and Zhang L. Combined laboratory and imaging indicators to construct risk models for predicting immunotherapy efficacy and prognosis in non-small cell lung cancer: an observational study (STROBE compliant). Medicine (Baltimore) 2025; 104: e45224.

Table S1. Schoenfeld residual test for the proportional hazards assumption in the multivariable Cox regression model

Variable	χ^2	df	*P* value
Global	12.21	10	0.272
Age	0.29	1	0.592
Sex	0.55	1	0.460
Stage	6.04	3	0.109
Histology	2.57	2	0.276
Liver metastasis	0.07	1	0.798
D-dimer change group	0.80	2	0.670

Based on the multivariable Cox regression model (N = 192; D-dimer change group referenced to Stable; liver metastasis referenced to absent; histology "Other" subgroup merged into Adenocarcinoma owing to zero events).

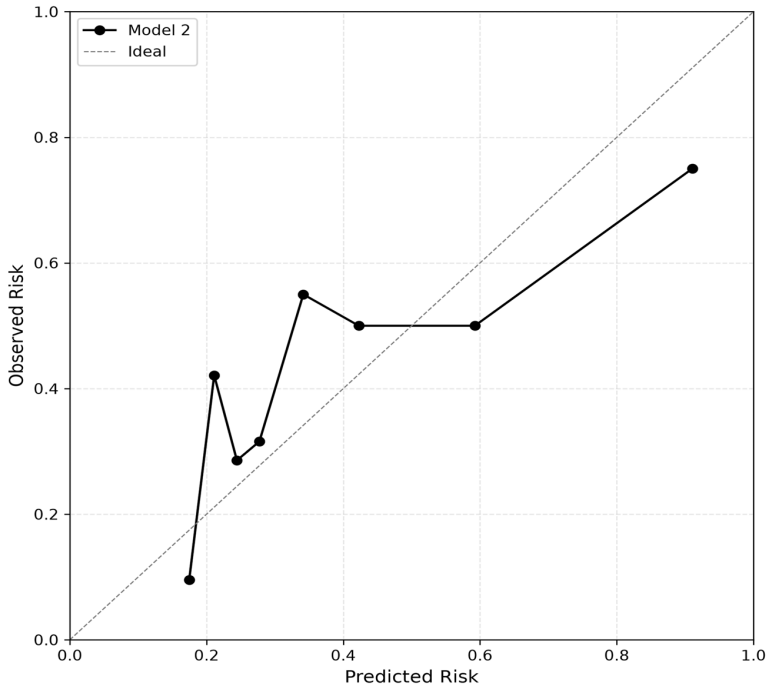

Figure S1. Calibration curve for 12-month overall survival. The x-axis represents predicted risk; the y-axis represents observed risk. The dashed diagonal line indicates perfect calibration (MAE = 0.013).

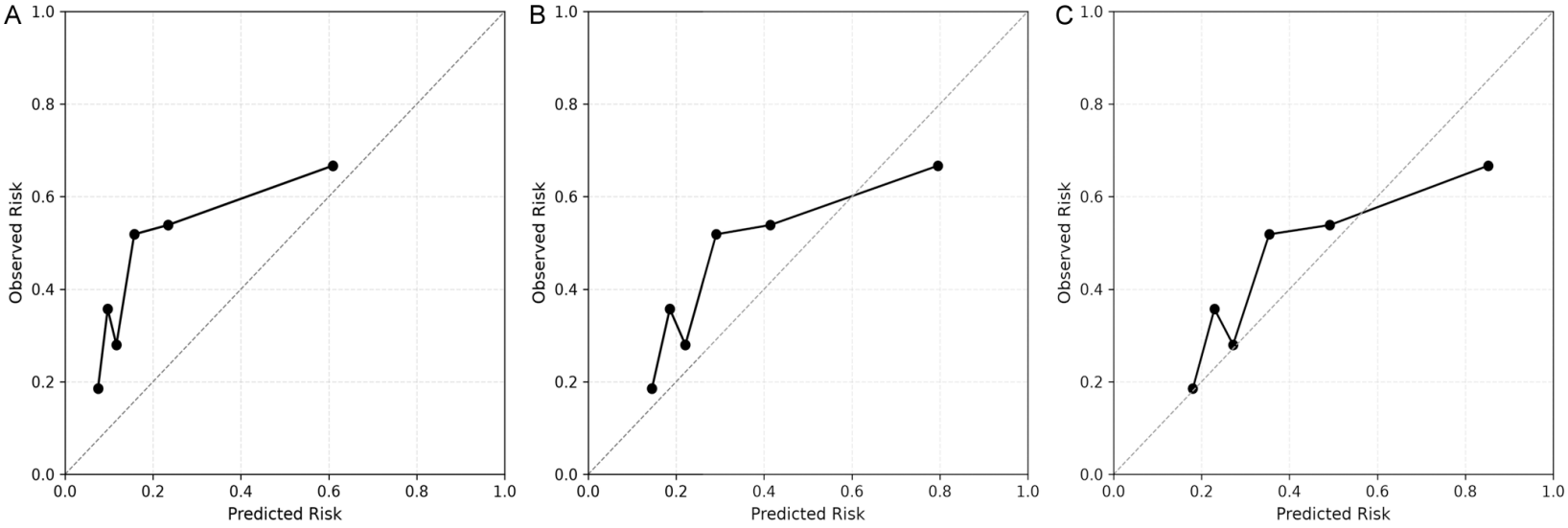

Figure S2. Multi-timepoint calibration of the combined coagulation-marker model at 6, 9, and 12 months after the 3-month landmark. Predicted versus observed overall survival probabilities are shown; points on the diagonal indicate perfect calibration.

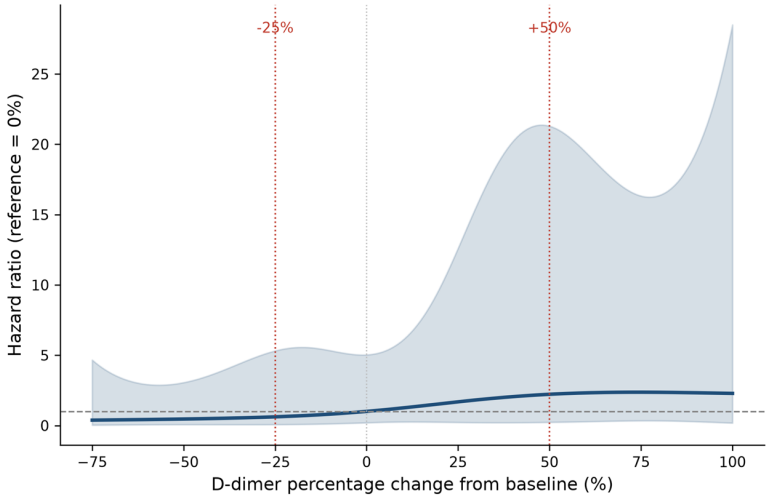

Figure S3. Restricted cubic spline analysis of the association between D-dimer percentage change and mortality risk. The solid line represents the estimated hazard ratio; the shaded band represents the 95% confidence interval. The non-linear relationship supports -25% and +50% as suitable clustering thresholds.

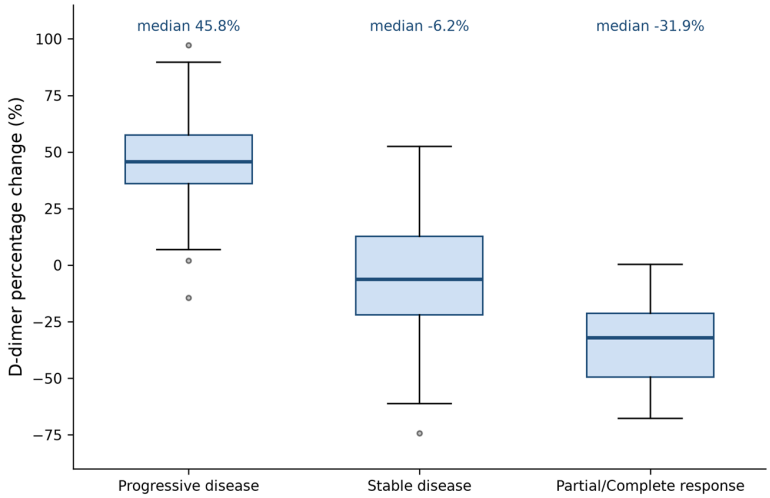

Figure S4. Distribution of D-dimer percentage change across RECIST response categories. The median D-dimer change was 45.8% in the progressive disease group, -6.2% in the stable disease group, and -31.9% in the partial/complete response group (Kruskal-Wallis test, $P < 0.001$).